Supplementary Material

Neighbourhood species richness and drought-tolerance traits modulate tree growth and δ13C responses to drought

Florian Schnabel, Kathryn E. Barry, Susanne Eckhardt, Joannès Guillemot, Heike Geilmann, Anja Kahl, Heiko Moossen, Jürgen Bauhus, Christian Wirth*

*Corresponding author: florian.schnabel@idiv.de

This file includes:

Figs. S1 to S12
Tables S1 to S18
Supplementary analysis 1
Supplementary discussion 1
References

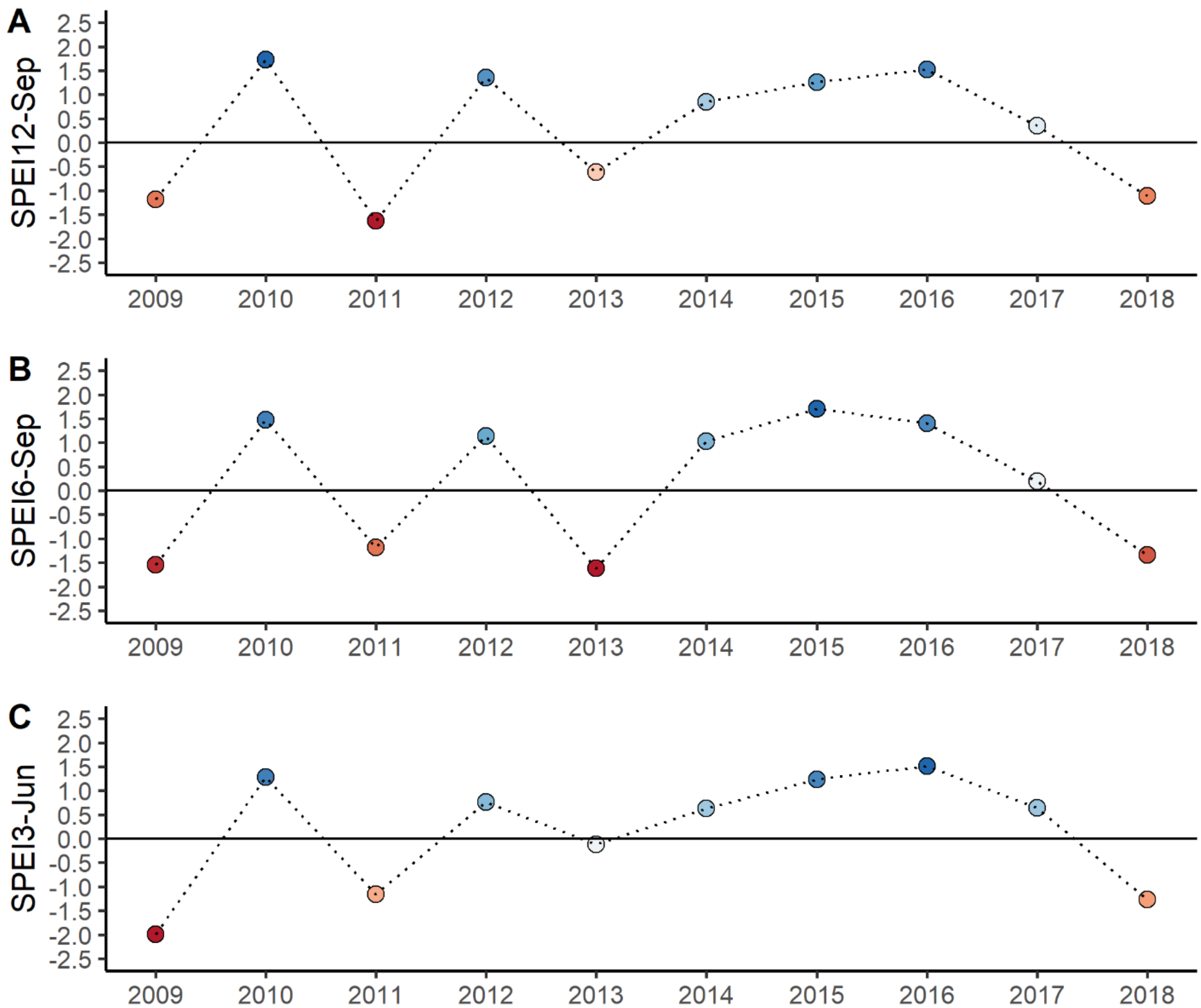

Fig. S1 Climate-based characterisation of the study years 2016 (wet), 2017 (intermediate) and 2018 (dry). Shown are standardised climatic water balances calculated based on the standardised precipitation evapotranspiration index (SPEI) (Vicente-Serrano, Beguería, & López-Moreno, 2010) calculated from a high-resolution time-series of interpolated climate station data (CRU TS v4.04; Harris, Osborn, Jones, & Lister, 2020). SPEIs are compared for the three months of the peak vegetation period (SPEI3, April-July) for the six months of the entire vegetation period (SPEI6, April-September) and the twelve months of a whole year since the end of the vegetation period of the preceding year (SPEI12, October-September), since the establishment of the BEF-China experiment (2009). The wet-to-dry study years are highlighted with a red circle. Blue points indicate wetter and red points drier conditions than the long-term mean (1901-2019); values below -1 and above 1 can be considered exceptional.

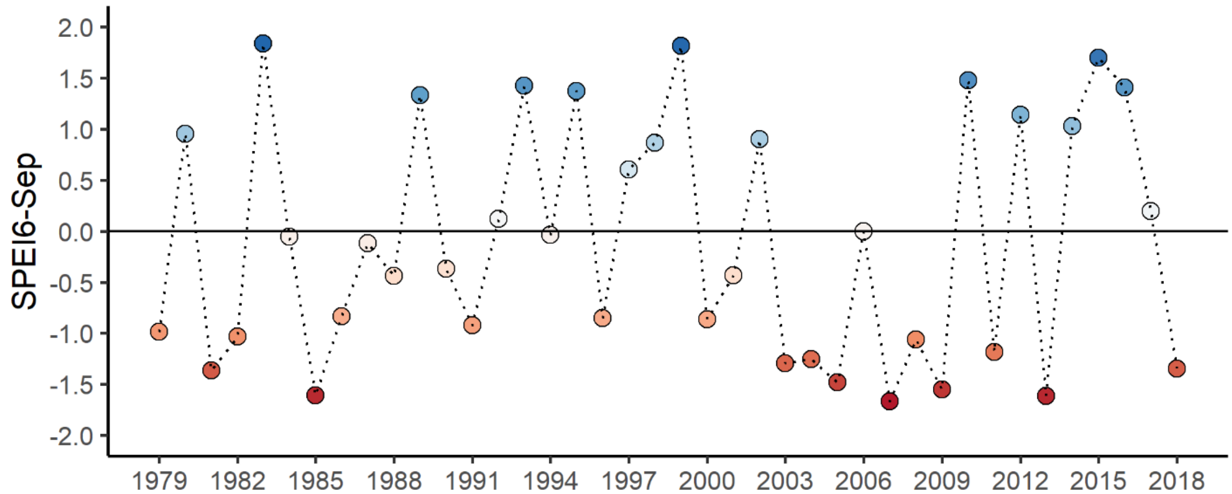

Fig. S2 A long-term perspective on standardized climatic water balances at our study site. Shown are values of the standardised precipitation evapotranspiration index (SPEI) for the principal vegetation period (April-September). For further details on the underlying data and SPEI calculation see methods and Fig.S1.

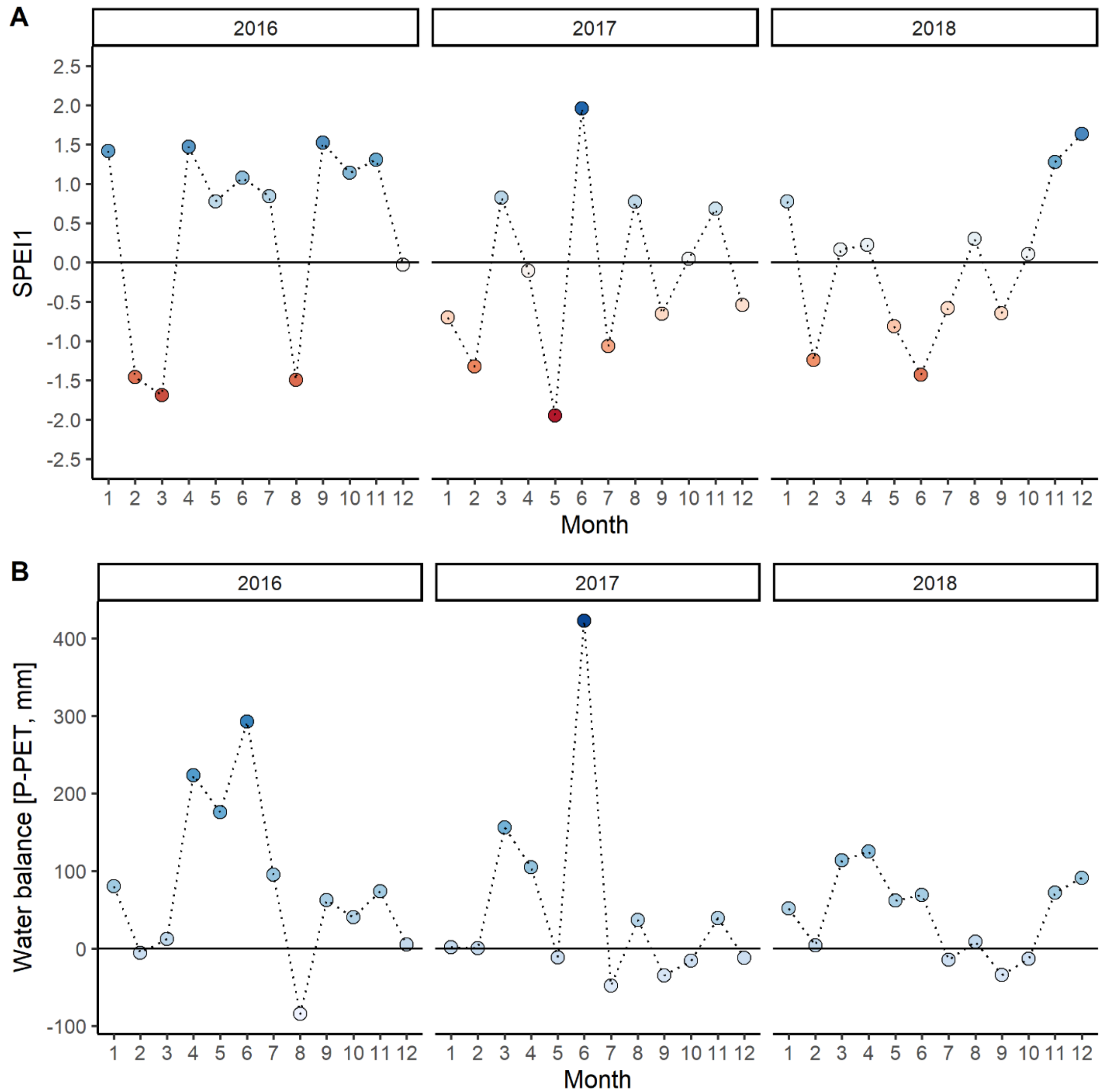

Fig. S3 Intra-annual climatic water balances at our study site. Shown are (A) values of the standardised precipitation evapotranspiration index (SPEI) and (B) non-standardized water balances of precipitation minus potential evapotranspiration (PET) for each month for the study years 2016-2018. For further details on the underlying data and SPEI calculation see methods and Fig.S1.

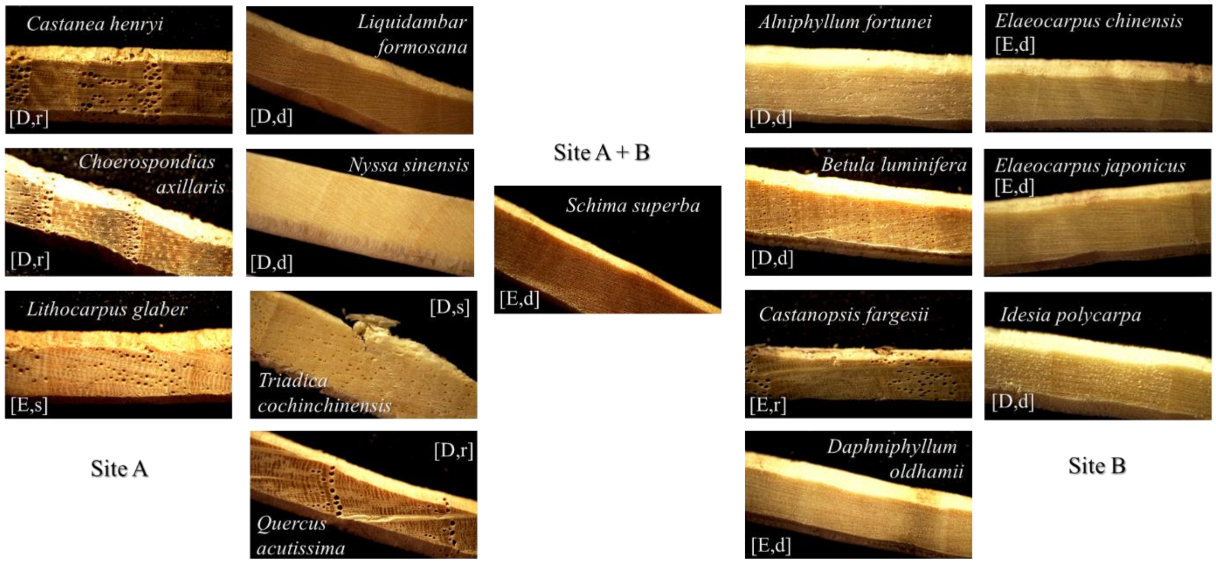

Fig. S4 Wood anatomy of the 15 tree species sampled in this study. Shown are photographs of exemplary cores per species and experimental site (see Table S1 for details on the species). Capital letters show the leaf habit (evergreen (E) and deciduous (D)) and lower-case letters wood porosity (ring porous (r), diffuse porous (d) and semi-ring porous (s)). Photographs were taken after surface preparation with a core microtome (Gärtner & Nievergelt, 2010).

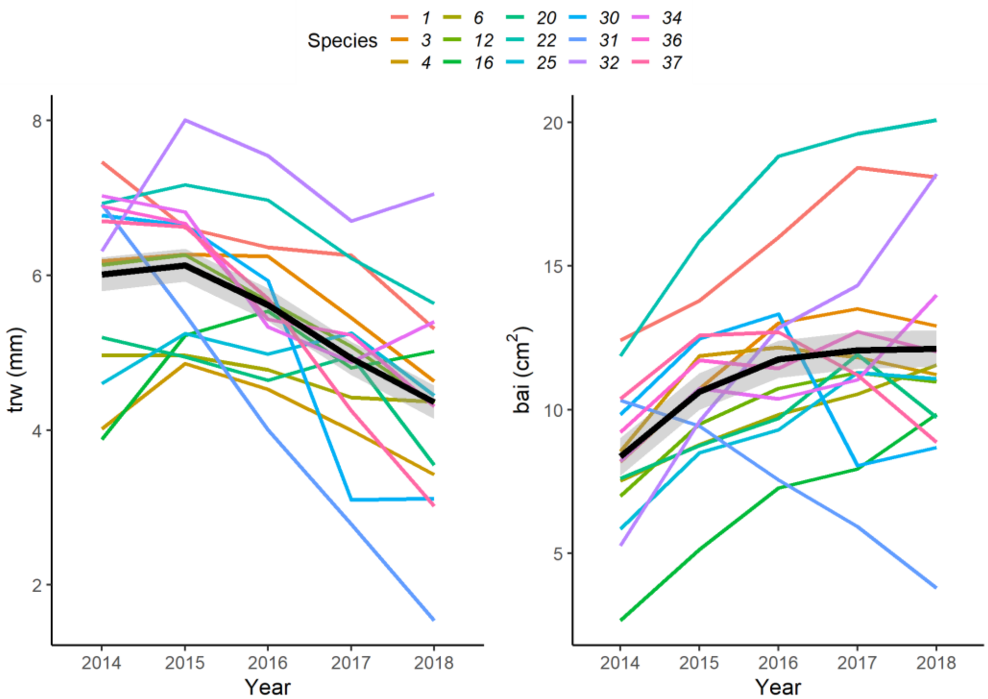

Fig. S5 Comparison of focal tree tree-ring width (trw, mm) and basal area increment (bai, cm^2) series.

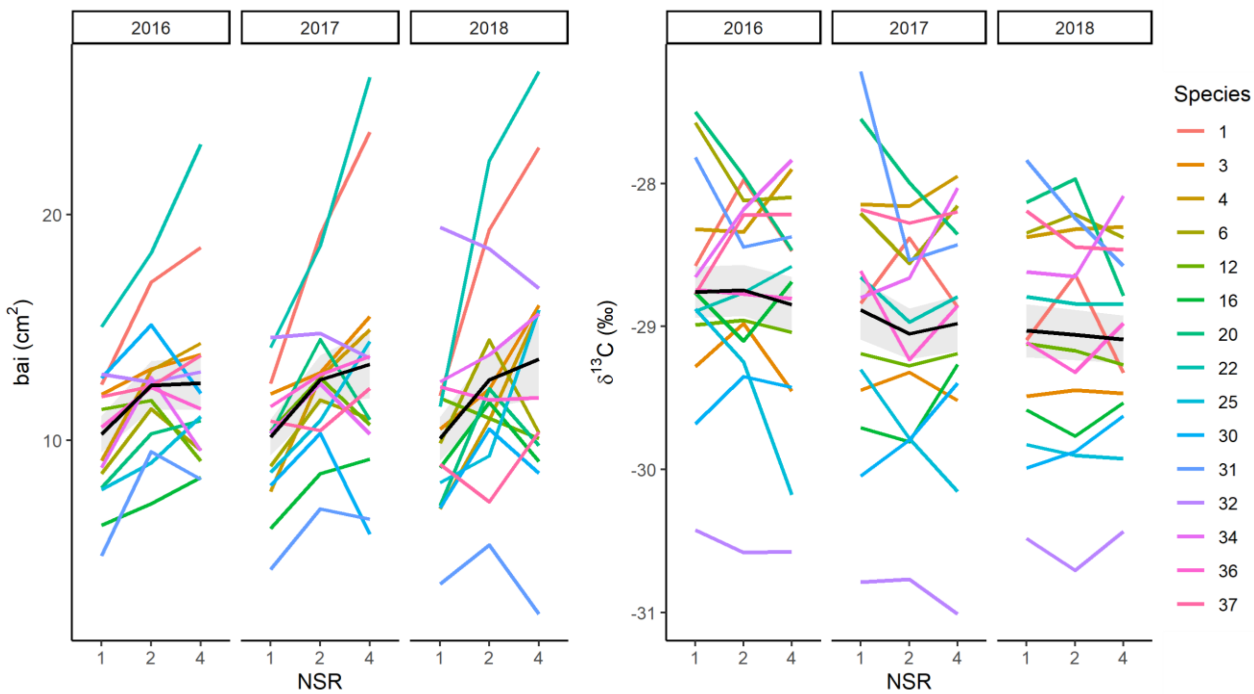

Fig. S6 Species-specific variability in focal tree growth (expressed as basal area increment, bai) and $\delta^{13}C$ in wood of focal trees per year and neighbourhood species richness (NSR) level. Coloured lines show mean values for each of the 15 studied species. Species identity is shown as species code; see species list in Table S1. The black line represents the fit of a simple linear regression across species to visualize overall trends; grey bands show a 95% confidence interval.

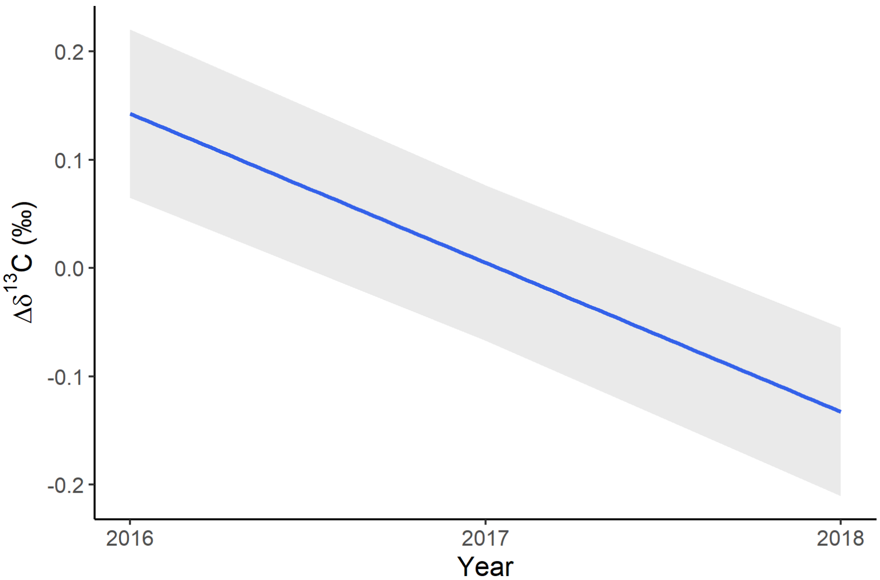

Fig. S7 Effect of study year on $\delta^{13}C$ in wood of focal trees. The blue line is a linear mixed-effects model fit and the grey band shows a 95% confidence interval. See Table S6 for details on the fitted model.

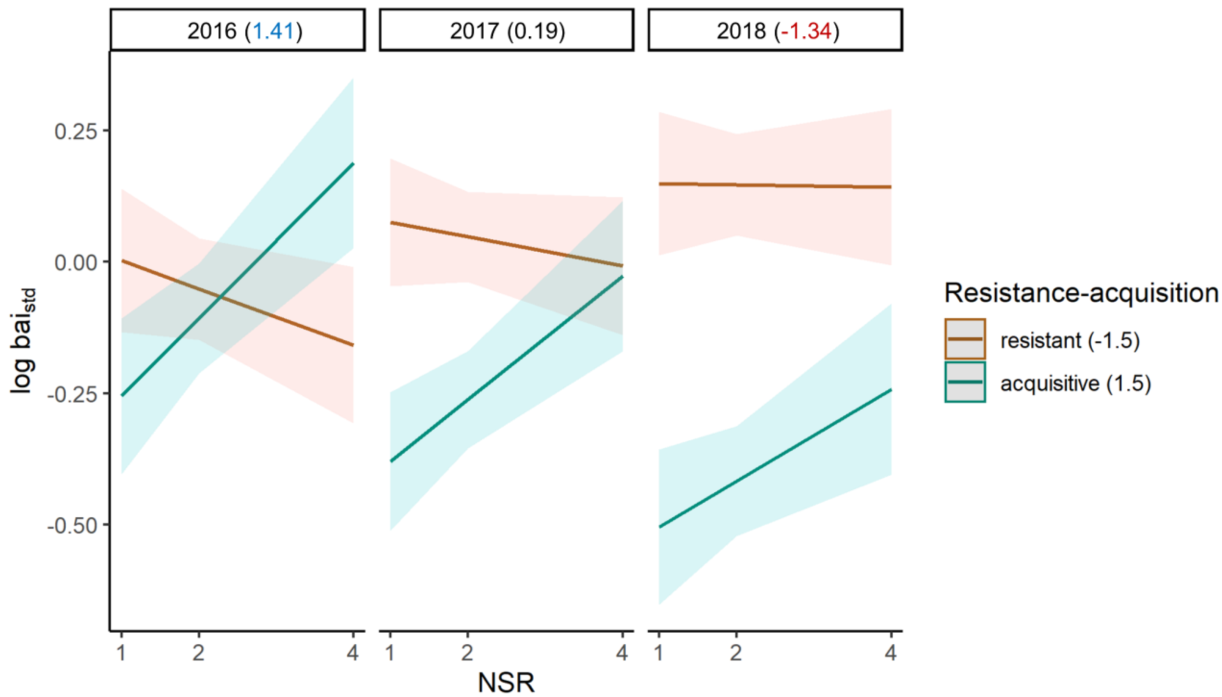

Fig. S8 Modulation of the relationship between neighbourhood species richness (NSR), climate and growth by resistance-acquisition traits. Lines represent linear mixed-effects model fits and coloured bands show a 95% confidence interval. The models depict marginally significant, interactive effects of NSR and study year (2016-2018 with wet-to-dry climate, SPEI values in brackets) on growth of focal trees predicted for cavitation resistant (PC1 value of -1.5) and for acquisitive focal trees (PC1 value of 1.5). See Fig. 1 for details on the study design and Table S10 for details on the fitted model.

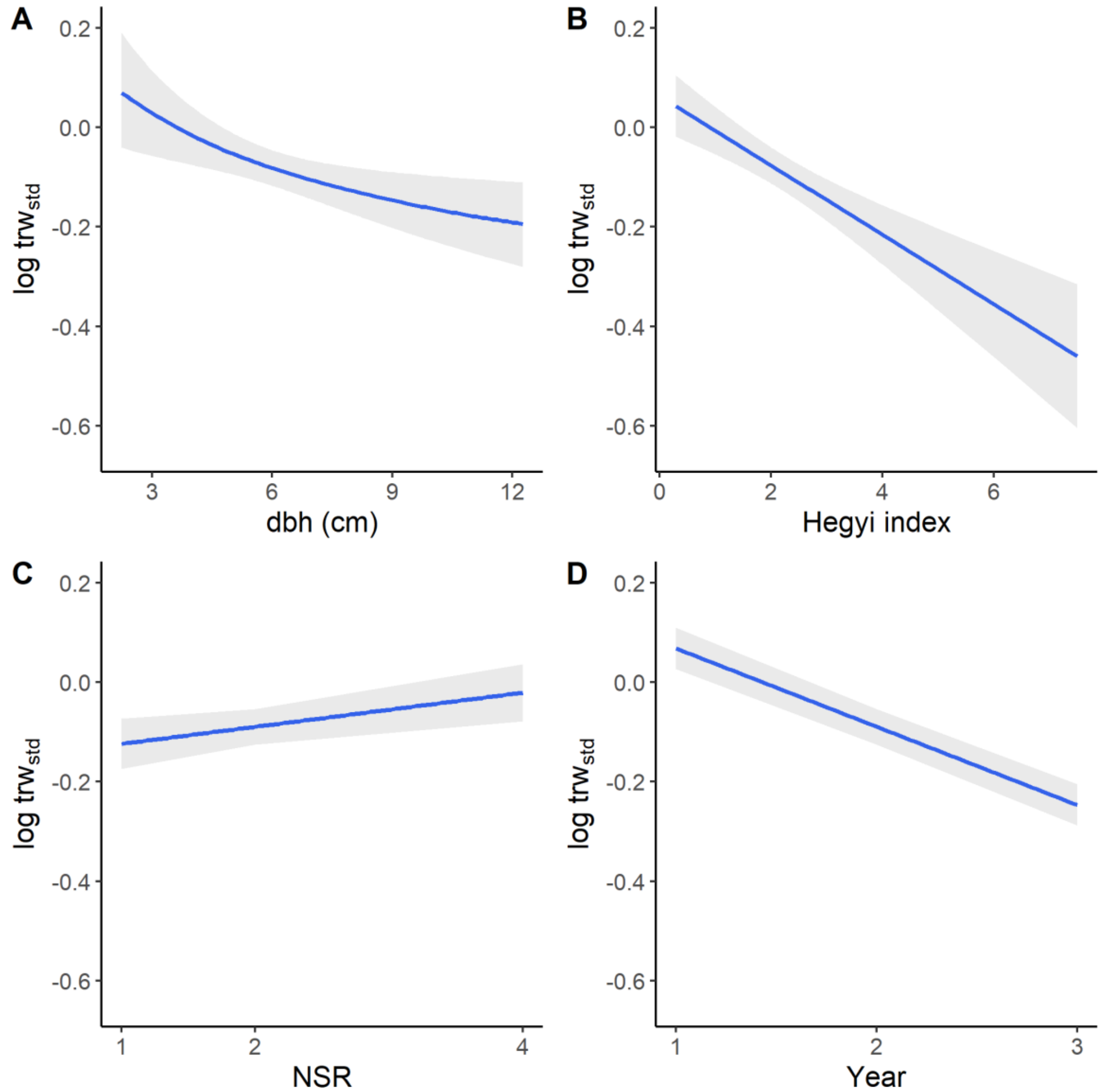

Fig. S9 Effects of tree size (dbh), neighbourhood competition (Hegyi index), neighbourhood species richness (NSR) and study year on the logarithm of tree-ring width (trw_{std}) of focal trees. The blue lines are linear mixed-effects model fits and the grey bands show a 95% confidence interval.

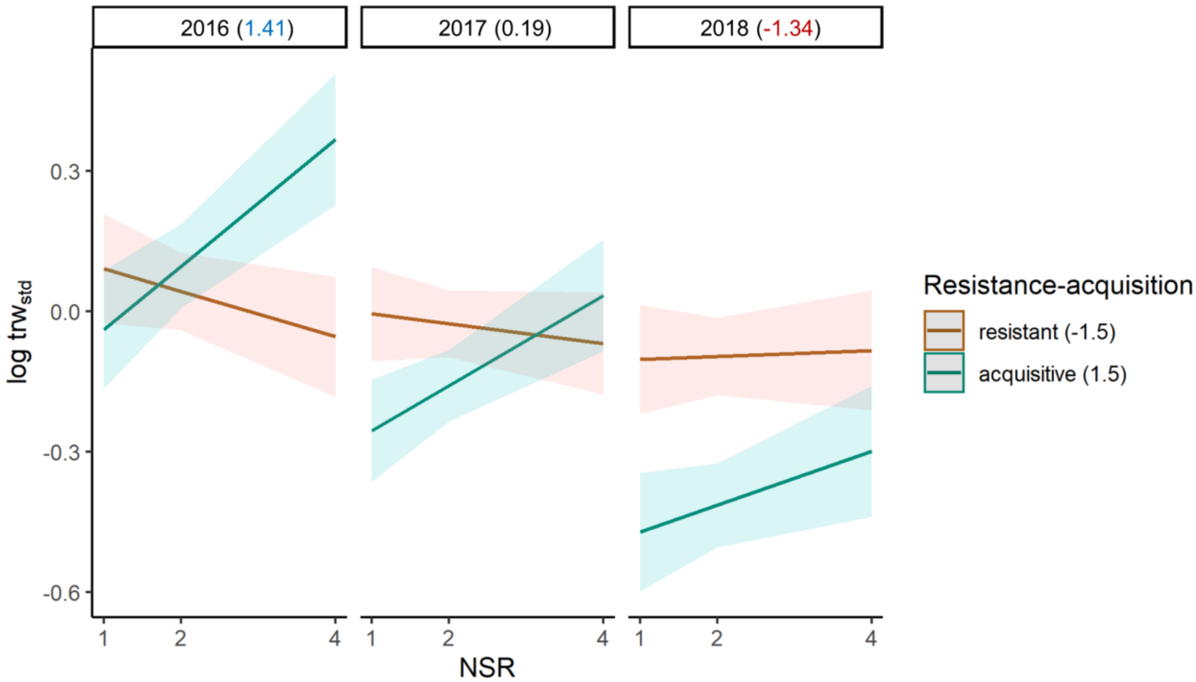

Fig. S10 Modulation of the relationship between neighbourhood species richness (NSR), climate and growth by resistance-acquisition traits using tree-ring width (trw_{std}) of focal trees instead of basal area increment (bai_{std}) as indicator of growth. Lines represent linear mixed-effects model fits and coloured bands show a 95% confidence interval. The model depicts significant, interactive effects of NSR and study year (2016-2018 with wet-to-dry climate, SPEI values in brackets) on growth predicted for cavitation resistant (PC1 value of -1.5) and for acquisitive focal trees (PC1 value of 1.5) (NSR × year × focal tree resistance-acquisition traits, $t = -2.21$, $P = 0.027$). See Fig. 1 for details on the study design.

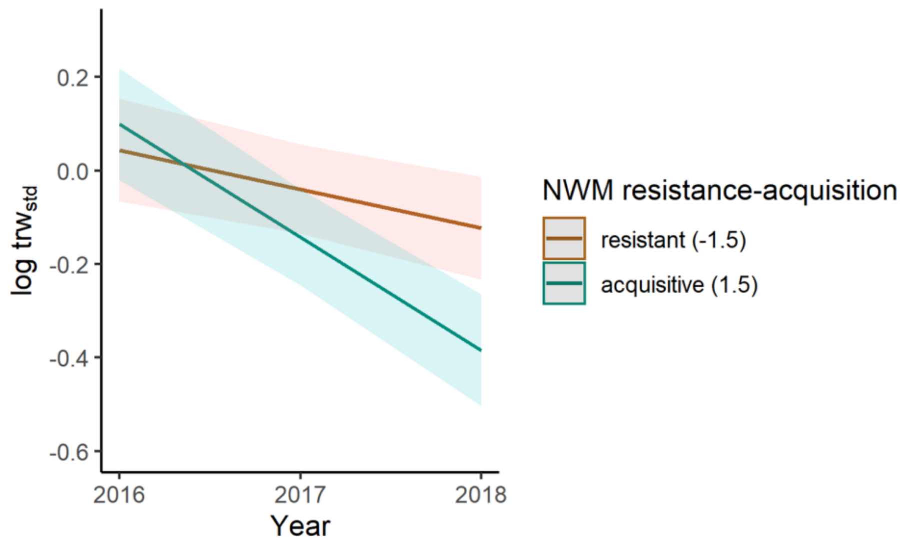

Fig. S11 Modulation of the relationship between climate and growth by the neighbourhood-weighted mean (NWM) of resistance-acquisition traits using tree-ring width (trw_{std}) of focal trees instead of basal area increment (bai_{std}) as indicator of growth. Lines represent linear mixed-effects model fits and coloured bands show a 95% confidence interval. The model depicts a significant effect of study year (2016-2018 with wet-to-dry climate, SPEI values in brackets) on the logarithm of trw_{std} predicted for a neighbourhood dominated by cavitation resistant (PC1 value of -1.5) and acquisitive species (PC1 value of 1.5) (year × NWM resistance-acquisition, $t = -2.90$, $P = 0.004$). See Fig. 1 for details on the study design.

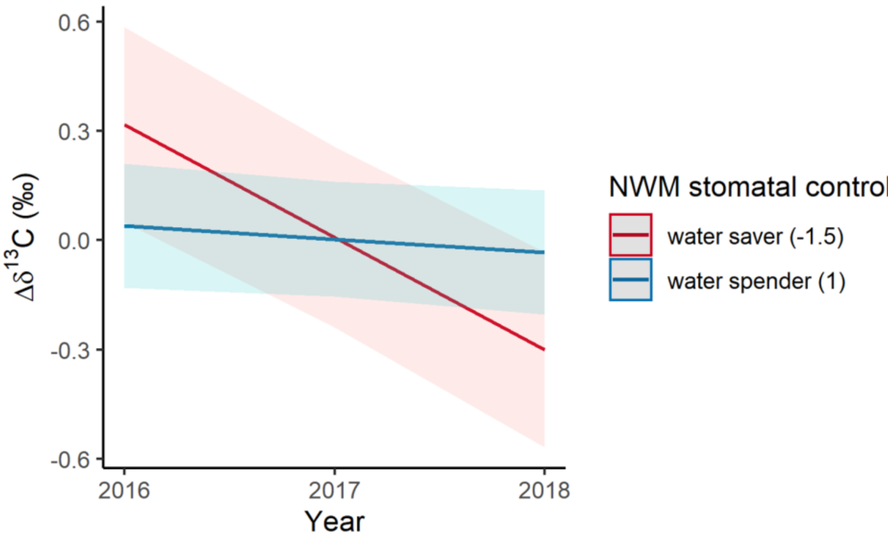

Fig. S12 Modulation of the relationship between climate and $\delta^{13}C$ by the neighbourhood-weighted mean (NWM) of stomatal control traits. Lines represent linear mixed-effects model fits and coloured bands show a 95% confidence interval. The model depicts a significant effect of study year (2016-2018 with wet-to-dry climate, SPEI values in brackets) on $\delta^{13}C$ in wood of focal trees predicted for a water saver (PC2 value of -1.5) and for a water spender (PC2 value of 1.0) dominated neighbourhood. The sketch illustrates that the NWM of stomatal control traits (tree neighbourhood) modulates the relationship. See Fig. 1 for details on the study design and Table S16 for details on the fitted model.

Table S1 The 40 broadleaved evergreen and deciduous tree species planted in BEF-China

Species names	Family	Species code	Leaf habit	Site
Acer davidii	*Sapindaceae*	27	D	A
Ailanthus altissima	*Simaroubaceae*	29	D	B
Alniphyllum fortunei	***Styracaceae***	**30**	**D**	**B**
Betula luminifera	***Betulaceae***	**31**	**D**	**B**
Castanea henryi	***Fagaceae***	**1**	**D**	**A**
Castanopsis carlesii	*Fagaceae*	10	E	A
Castanopsis eyrei	*Fagaceae*	13	E	AB
Castanopsis fargesii	***Fagaceae***	**32**	**E**	**B**
Castanopsis sclerophylla	*Fagaceae*	14	E	AB
Celtis biondii	*Cannabaceae*	33	D	B
Choerospondias axillaris	***Anacardiaceae***	**4**	**D**	**A**
Cinnamomum camphora	*Lauraceae*	17	E	AB
Cyclobalanopsis glauca	*Fagaceae*	11	E	AB
Cyclobalanopsis myrsinifolia	*Fagaceae*	9	E	A
Daphniphyllum oldhamii	***Daphniphyllaceae***	**16**	**E**	**AB***
Diospyros japonica	*Ebenaceae*	15	D	AB
Elaeocarpus chinensis	***Elaeocarpaceae***	**34**	**E**	**B**
Elaeocarpus glabripetalus	*Elaeocarpaceae*	35	E	B
Elaeocarpus japonicus	***Elaeocarpaceae***	**36**	**E**	**B**
Idesia polycarpa	***Salicaceae***	**37**	**D**	**B**
Koelreuteria bipinnata	*Sapindaceae*	18	D	A
Liquidambar formosana	***Altingiaceae***	**6**	**D**	**A**
Lithocarpus glaber	***Fagaceae***	**12**	**E**	**A*B**
Machilus grijsii	*Lauraceae*	39	E	B
Machilus leptophylla	*Lauraceae*	41	E	B
Machilus thunbergii	*Lauraceae*	40	E	B
Manglietia fordiana	*Magnoliaceae*	42	E	B
Melia azedarach	*Meliaceae*	26	D	A
Meliosma flexuosa	*Sabiaceae*	38	D	B
Nyssa sinensis	***Cornaceae***	**20**	**D**	**A**
Phoebe bournei	*Lauraceae*	43	E	B
Quercus acutissima	***Fagaceae***	**25**	**D**	**A**
Quercus fabri	*Fagaceae*	24	D	A
Quercus phillyreoides	*Fagaceae*	44	E	B
Quercus serrata	*Fagaceae*	8	D	A
Rhus chinensis	*Anacardiaceae*	23	D	A
Sapindus saponaria	*Sapindaceae*	19	D	A
Triadica cochinchinensis	***Euphorbiaceae***	**22**	**D**	**A**
Triadica sebifera	*Euphorbiaceae*	21	D	A
Schima superba	***Theaceae***	**3**	**E**	**A*B***

Note: Species from which tree cores were extracted are highlighted in bold (see Fig. 1 for the species selection). Shown are species and family names, the species identity codes used in Fig. 1, leaf habit (E, evergreen; D, Deciduous) and the site at which the species were planted. In case of species planted at both sites, asterisks indicate at which site the species was sampled. For more details on the tree species taxonomy, their characteristics and the experimental design see Bruelheide et al., 2014; Huang et al., 2018.

Table S2 Resistance-acquisition and stomatal control traits were used in this study (adapted from Schnabel et al., 2021).

Abbreviation	**Trait description**	**Unit**
Ψ_{50}	Water potential at which 50% initial conductivity is lost	MPa
SLA	Specific leaf area	m^2 kg^{-1}
LEAFT	Leaf toughness	N mm^{-1}
CN	Carbon to nitrogen ratio	Ratio
CONMAXFIT	Modelled maximum stomatal conductance	Non-dimensional
STOMDENS	Stomatal density	1 mm^{-2}
STOIND	Product of STODENS and stomatal size in μm^2	ratio
VPDMAXFIT	Vapor pressure deficit (VPD) at CONMAXFIT	hPA
VPDPOI	VPD at the point of inflection of modelled stomatal conductance	hPA

Note: Traits were measured in the BEF-China experiment and were used to calculate species level mean trait values by Kröber and Bruelheide (2014) and Kröber, Zhang, Ehmig, and Bruelheide (2014). See these studies and Schnabel et al. (2021) for detailed information on the individual traits and the two orthogonal drought-tolerance trait gradients they represent. Stomatal sensitivity is inferred here from modelled g_s~VPD curves through extracting the point at which a species starts to lower its stomatal conductance (the VPD at maximum stomatal conductance, VPDMAXFIT) and the point where the slope of the curve turns from positive to negative (VPDPOI), which is a measure of how fast stomatal close under increasing VPD.

Table S3 Description of competition indices.

Index	Description
nhigher	Number of neighbours higher than the focal tree
relbah	Basal area of neighbours higher than the focal tree
relbab	Basal area of neighbours with higher basal area than the focal tree
hegyi	Hegyi index including all neighbours
hegyih	Hegyi index of neighbours higher than the focal tree
hegyib	Hegyi index of neighbours with higher basal area than the focal tree
hcom	Summed height of neighbours relative to the focal tree

Notes: We modelled distance depended competition effects of neighbouring trees on focal trees using the Hegyi index (e.g. Mailly, Turbis, & Pothier, 2003) with the following formula when including all neighbours: $hegyi = \sum_{c=1}^{n} \frac{ba_c}{ba_t} * \frac{1}{d_{tc}}$; where *ba* is the basal area of either the focal tree *t* or its competitor *c* and d_{tc} the distance between focal tree and neighbour. We subsequently adjusted this formula to only include those neighbours higher than the focal tree or those with a higher basal area than the focal tree.

Table S4 Best-fitting trait-independent linear mixed-effects model after model selection.

		log(bai$_{std}$)			
Predictors	*Estimates*	*CI*	*Statistic*	*p*	*df*
(Intercept)	-0.19	-0.29 – -0.10	-4.18	**<0.001**	119.74
dbh	0.10	0.06 – 0.14	5.01	**<0.001**	273.26
hegyi	-0.12	-0.15 – -0.08	-5.91	**<0.001**	328.58
NSR	0.04	0.01 – 0.08	2.29	**0.024**	120.00
Random Effects					
σ^2	0.09				
$\tau_{00\ tag:(plot\_no:site)}$	0.07				
$\tau_{00\ plot\_no:site}$	0.02				
ICC	0.51				
N $_{tag}$	336				
N $_{plot\_no}$	114				
N $_{site}$	2				
Observations	1008				
Marginal R^2 / Conditional R^2	0.155 / 0.585				

Note: Significant fixed effects printed in bold. Linear mixed-effects models (LMMs) fit with the packages lme4 (Bates, Mächler, Bolker, & Walker, 2015) and lmerTest (Kuznetsova, Brockhoff, & Christensen, 2017) in R using restricted maximum likelihood estimation (REML) and an α of 0.05 for reporting significant effects. Model tables including fixed and random effects as well as R^2 values were created using the sjPlot package (see Lüdecke (2021) for details). The model statistics, p-values, standard errors and confidence intervals (CI; 95%) were computed using Satterthwaite's approximation for degrees of freedom. 'Plot no' is the plot identifier and 'tag' the tree identifier. All analyses were conducted in R version 4.1.2 (R Core Team, 2021).

Table S5 Comparison of competition indices (Table S3) for the growth linear mixed-effects model (Table S4) against a null model without a competition index.

Model	npar	AIC	BIC	logLik	deviance	Chisq	Df	Pr(>Chisq)
null	6	912.56	942.05	-450.28	900.56	NA	NA	NA
nhigher	7	914.23	948.64	-450.11	900.23	0.33	1	0.57
relbah	7	913.18	947.59	-449.59	899.18	1.05	0	NA
relbab	7	904.85	939.26	-445.43	890.85	8.33	0	NA
hegyi	7	880.98	915.39	-433.49	866.98	23.87	0	NA
hegyih	7	909.19	943.6	-447.59	895.19	0	0	NA
hegyib	7	890.65	925.06	-438.32	876.65	18.54	0	NA
hcom	7	914.14	948.55	-450.07	900.14	0	0	NA

Table S6 Best-fitting trait-independent linear mixed-effects model after model selection.

	$\Delta\delta^{13}C$				
Predictors	*Estimates*	*CI*	*Statistic*	*p*	*df*
(Intercept)	0.28	0.19 – 0.37	5.89	**<0.001**	256.95
year int	-0.14	-0.17 – -0.11	-9.06	**<0.001**	671.00
Random Effects					
σ^2	0.16				
$\tau_{00\ tag:(plot\_no:site)}$	0.29				
$\tau_{00\ plot\_no:site}$	0.03				
ICC	0.67				
N_{tag}	336				
N_{plot_no}	114				
N_{site}	2				
Observations	1008				
Marginal R^2 / Conditional R^2	0.026 / 0.683				

Note: Significant fixed effects printed in bold. Linear mixed-effects models (LMMs) fit with the packages lme4 (Bates et al., 2015) and lmerTest (Kuznetsova et al., 2017) in R using restricted maximum likelihood estimation (REML) and an α of 0.05 for reporting significant effects. Model tables including fixed and random effects as well as R^2 values were created using the sjPlot package (see Lüdecke (2021) for details). The model statistics, p-values, standard errors and confidence intervals (CI; 95%) were computed using Satterthwaite's approximation for degrees of freedom. 'Plot no' is the plot identifier and 'tag' the tree identifier. All analyses were conducted in R version 4.1.2 (R Core Team, 2021).

Table S7 Comparison of competition indices (Table S3) for the $\delta^{13}C$ linear mixed-effects model (Table S6) against a null model without a competition index.

Models	npar	AIC	BIC	logLik	deviance	Chisq	Df	Pr(>Chisq)
null	5	1650.47	1675.04	-820.23	1640.47	NA	NA	NA
nhigher	6	1652.22	1681.71	-820.11	1640.22	0.25	1	0.62
relbah	6	1650.80	1680.30	-819.40	1638.80	1.41	0	NA
relbab	6	1652.09	1681.59	-820.05	1640.09	0.00	0	NA
hegyi	6	1651.34	1680.83	-819.67	1639.34	0.75	0	NA
hegyih	6	1650.72	1680.22	-819.36	1638.72	0.61	0	NA
hegyib	6	1652.38	1681.88	-820.19	1640.38	0.00	0	NA
hcom	6	1652.44	1681.94	-820.22	1640.44	0.00	0	NA

Table S8 Best-fitting linear mixed-effects model of focal tree resistance-acquisition traits after model selection.

	log(bai_{std})				
Predictors	*Estimates*	*CI*	*Statistic*	*p*	*df*
(Intercept)	-0.15	-0.25 – -0.06	-3.13	**0.002**	178.59
dbh	0.12	0.08 – 0.16	5.80	**<0.001**	276.94
hegyi	-0.12	-0.16 – -0.08	-6.06	**<0.001**	324.39
NSR	0.04	0.01 – 0.07	2.40	**0.018**	116.73
resistance-acquisition	-0.02	-0.11 – 0.08	-0.31	0.758	193.94
year int	-0.02	-0.04 – 0.00	-1.79	0.074	670.00
NSR * resistance-acquisition	0.04	0.01 – 0.07	2.45	**0.015**	160.99
resistance-acquisition * year int	-0.08	-0.10 – -0.05	-6.84	**<0.001**	670.00
Random Effects					
σ^2	0.08				
τ_{00} tag:(plot_no:site)	0.07				
τ_{00} plot_no:site	0.01				
ICC	0.52				
N_{tag}	336				
N_{plot_no}	114				
N_{site}	2				
Observations	1008				
Marginal R^2 / Conditional R^2	0.200 / 0.612				

Note: Significant fixed effects printed in bold. Linear mixed-effects models (LMMs) fit with the packages lme4 (Bates et al., 2015) and lmerTest (Kuznetsova et al., 2017) in R using restricted maximum likelihood estimation (REML) and an α of 0.05 for reporting significant effects. Model tables including fixed and random effects as well as R^2 values were created using the sjPlot package (see Lüdecke (2021) for details). The model statistics, p-values, standard errors and confidence intervals (CI; 95%) were computed using Satterthwaite's approximation for degrees of freedom. 'Plot no' is the plot identifier and 'tag' the tree identifier. All analyses were conducted in R version 4.1.2 (R Core Team, 2021).

Table S9 Best-fitting linear mixed-effects model of neighbour resistance-acquisition traits after model selection.

	log(bai$_{std}$)				
Predictors	*Estimates*	*CI*	*Statistic*	*p*	*df*
(Intercept)	-0.15	-0.25 – -0.05	-2.88	**0.004**	176.14
dbh	0.12	0.08 – 0.16	5.58	**<0.001**	282.81
hegyi	-0.12	-0.16 – -0.08	-6.07	**<0.001**	324.78
NSR	0.04	0.00 – 0.07	2.12	**0.036**	115.21
year int	-0.02	-0.04 – 0.00	-1.75	0.080	670.00
resistance-acquisition	0.03	-0.03 – 0.10	1.08	0.282	490.68
year int * resistance-acquisition	-0.05	-0.07 – -0.02	-4.17	**<0.001**	670.00
Random Effects					
σ^2	0.09				
$\tau_{00\ tag:(plot\_no:site)}$	0.07				
$\tau_{00\ plot\_no:site}$	0.02				
ICC	0.51				
N $_{tag}$	336				
N $_{plot\_no}$	114				
N $_{site}$	2				
Observations	1008				
Marginal R^2 / Conditional R^2	0.173 / 0.595				

Note: Significant fixed effects printed in bold. Linear mixed-effects models (LMMs) fit with the packages lme4 (Bates et al., 2015) and lmerTest (Kuznetsova et al., 2017) in R using restricted maximum likelihood estimation (REML) and an α of 0.05 for reporting significant effects. Model tables including fixed and random effects as well as R^2 values were created using the sjPlot package (see Lüdecke (2021) for details). The model statistics, p-values, standard errors and confidence intervals (CI; 95%) were computed using Satterthwaite's approximation for degrees of freedom. 'Plot no' is the plot identifier and 'tag' the tree identifier. All analyses were conducted in R version 4.1.2 (R Core Team, 2021).

Table S10 Linear mixed-effects model of focal tree resistance-acquisition traits that still includes the marginally significant 3-way interaction between year, neighbourhood species richness (NSR) and resistance-acquisition traits.

	log(bai_{std})				
Predictors	*Estimates*	*CI*	*Statistic*	*p*	*df*
(Intercept)	-0.16	-0.28 – -0.03	-2.43	**0.015**	425.58
dbh	0.12	0.08 – 0.16	5.80	**<0.001**	276.94
hegyi	-0.12	-0.16 – -0.08	-6.06	**<0.001**	324.39
NSR	0.04	-0.01 – 0.09	1.68	0.093	428.37
year int	-0.02	-0.06 – 0.03	-0.80	0.422	668.00
resistance-acquisition	-0.09	-0.21 – 0.04	-1.35	0.177	451.55
NSR * year int	-0.00	-0.02 – 0.02	-0.05	0.963	668.00
NSR * resistance-acquisition	0.07	0.02 – 0.12	2.95	**0.003**	566.08
year int * resistance-acquisition	-0.04	-0.09 – 0.01	-1.68	0.093	668.00
(NSR * year int) * resistance-acquisition	-0.02	-0.03 – 0.00	-1.75	0.080	668.00
Random Effects					
σ^2	0.08				
τ_{00} tag:(plot_no:site)	0.07				
τ_{00} plot_no:site	0.01				
ICC	0.52				
N tag	336				
N plot_no	114				
N site	2				
Observations	1008				
Marginal R^2 / Conditional R^2	0.201 / 0.613				

Note: Significant fixed effects printed in bold. Linear mixed-effects models (LMMs) fit with the packages lme4 (Bates et al., 2015) and lmerTest (Kuznetsova et al., 2017) in R using restricted maximum likelihood estimation (REML) and an α of 0.05 for reporting significant effects. Model tables including fixed and random effects as well as R^2 values were created using the sjPlot package (see Lüdecke (2021) for details). The model statistics, p-values, standard errors and confidence intervals (CI; 95%) were computed using Satterthwaite's approximation for degrees of freedom. ‘Plot no’ is the plot identifier and ‘tag’ the tree identifier. All analyses were conducted in R version 4.1.2 (R Core Team, 2021).

Table S11 Best-fitting linear mixed-effects model of focal tree stomatal control traits after model selection.

	log(bai$_{std}$)				
Predictors	*Estimates*	*CI*	*Statistic*	*p*	*df*
(Intercept)	-0.16	-0.26 – -0.05	-3.00	**0.003**	177.35
dbh	0.10	0.06 – 0.14	5.02	**<0.001**	274.02
hegyi	-0.12	-0.15 – -0.08	-5.89	**<0.001**	327.59
NSR	0.04	0.01 – 0.08	2.29	**0.024**	118.62
year int	-0.02	-0.04 – 0.00	-1.77	0.078	670.00
stomatal control	0.10	0.04 – 0.17	3.37	**0.001**	503.88
year int * stomatal control	-0.06	-0.08 – -0.04	-5.10	**<0.001**	670.00
Random Effects					
σ^2	0.08				
$\tau_{00\ tag:(plot\_no:site)}$	0.07				
$\tau_{00\ plot\_no:site}$	0.02				
ICC	0.52				
N_{tag}	336				
N_{plot_no}	114				
N_{site}	2				
Observations	1008				
Marginal R^2 / Conditional R^2	0.166 / 0.603				

Note: Significant fixed effects printed in bold. Linear mixed-effects models (LMMs) fit with the packages lme4 (Bates et al., 2015) and lmerTest (Kuznetsova et al., 2017) in R using restricted maximum likelihood estimation (REML) and an α of 0.05 for reporting significant effects. Model tables including fixed and random effects as well as R^2 values were created using the sjPlot package (see Lüdecke (2021) for details). The model statistics, p-values, standard errors and confidence intervals (CI; 95%) were computed using Satterthwaite's approximation for degrees of freedom. 'Plot no' is the plot identifier and 'tag' the tree identifier. All analyses were conducted in R version 4.1.2 (R Core Team, 2021).

Table S12 Best-fitting linear mixed-effects model of neighbour stomatal control traits after model selection.

	$\log(bai_{std})$				
Predictors	*Estimates*	*CI*	*Statistic*	*p*	*df*
(Intercept)	-0.15	-0.26 – -0.05	-2.95	**0.004**	179.65
dbh	0.10	0.06 – 0.14	4.95	**<0.001**	275.70
hegyi	-0.12	-0.16 – -0.08	-5.92	**<0.001**	328.73
NSR	0.04	0.00 – 0.07	2.23	**0.027**	119.44
year int	-0.02	-0.04 – 0.00	-1.74	0.082	670.00
stomatal control	0.08	0.02 – 0.14	2.57	**0.011**	502.83
year int * stomatal control	-0.03	-0.06 – -0.01	-3.04	**0.002**	670.00
Random Effects					
σ^2	0.09				
$\tau_{00\ tag:(plot\_no:site)}$	0.07				
$\tau_{00\ plot\_no:site}$	0.02				
ICC	0.52				
N_{tag}	336				
N_{plot_no}	114				
N_{site}	2				
Observations	1008				
Marginal R^2 / Conditional R^2	0.160 / 0.593				

Note: Significant fixed effects printed in bold. Linear mixed-effects models (LMMs) fit with the packages lme4 (Bates et al., 2015) and lmerTest (Kuznetsova et al., 2017) in R using restricted maximum likelihood estimation (REML) and an α of 0.05 for reporting significant effects. Model tables including fixed and random effects as well as R^2 values were created using the sjPlot package (see Lüdecke (2021) for details). The model statistics, p-values, standard errors and confidence intervals (CI; 95%) were computed using Satterthwaite's approximation for degrees of freedom. 'Plot no' is the plot identifier and 'tag' the tree identifier. All analyses were conducted in R version 4.1.2 (R Core Team, 2021).

Table S13 Best-fitting linear mixed-effects model of focal tree resistance-acquisition traits after model selection.

	$\Delta\delta^{13}C$				
Predictors	*Estimates*	*CI*	*Statistic*	*p*	*df*
(Intercept)	0.16	0.08 – 0.24	3.91	**<0.001**	140.98
year cat [2017]	-0.19	-0.25 – -0.13	-6.21	**<0.001**	668.00
year cat [2018]	-0.28	-0.33 – -0.22	-9.14	**<0.001**	668.00
resistance-acquisition	-0.06	-0.14 – 0.02	-1.51	0.133	192.66
year cat [2017] * resistance-acquisition	0.11	0.05 – 0.16	3.51	**<0.001**	668.00
year cat [2018] * resistance-acquisition	0.06	-0.00 – 0.11	1.84	0.066	668.00
Random Effects					
σ^2	0.15				
$\tau_{00\ tag:(plot\_no:site)}$	0.29				
$\tau_{00\ plot\_no:site}$	0.04				
ICC	0.68				
N_{tag}	336				
N_{plot_no}	114				
N_{site}	2				
Observations	1008				
Marginal R^2 / Conditional R^2	0.031 / 0.690				

Note: Significant fixed effects printed in bold. Linear mixed-effects models (LMMs) fit with the packages lme4 (Bates et al., 2015) and lmerTest (Kuznetsova et al., 2017) in R using restricted maximum likelihood estimation (REML) and an α of 0.05 for reporting significant effects. Model tables including fixed and random effects as well as R^2 values were created using the sjPlot package (see Lüdecke (2021) for details). The model statistics, p-values, standard errors and confidence intervals (CI; 95%) were computed using Satterthwaite's approximation for degrees of freedom. 'Plot no' is the plot identifier and 'tag' the tree identifier. All analyses were conducted in R version 4.1.2 (R Core Team, 2021).

Table S14 Best-fitting linear mixed-effects model of neighbour resistance-acquisition traits after model selection.

	$\Delta\delta^{13}C$				
Predictors	*Estimates*	*CI*	*Statistic*	*p*	*df*
(Intercept)	0.16	0.08 – 0.24	3.92	**<0.001**	139.09
year cat [2017]	-0.19	-0.25 – -0.13	-6.24	**<0.001**	668.00
year cat [2018]	-0.28	-0.33 – -0.22	-9.19	**<0.001**	668.00
resistance-acquisition	-0.05	-0.13 – 0.03	-1.22	0.224	151.57
year cat [2017] * resistance-acquisition	0.13	0.07 – 0.19	4.35	**<0.001**	668.00
year cat [2018] * resistance-acquisition	0.07	0.01 – 0.13	2.27	**0.023**	668.00
Random Effects					
σ^2	0.15				
$\tau_{00\ tag:(plot\_no:site)}$	0.29				
$\tau_{00\ plot\_no:site}$	0.03				
ICC	0.68				
N_{tag}	336				
N_{plot_no}	114				
N_{site}	2				
Observations	1008				
Marginal R^2 / Conditional R^2	0.033 / 0.692				

Note: Significant fixed effects printed in bold. Linear mixed-effects models (LMMs) fit with the packages lme4 (Bates et al., 2015) and lmerTest (Kuznetsova et al., 2017) in R using restricted maximum likelihood estimation (REML) and an α of 0.05 for reporting significant effects. Model tables including fixed and random effects as well as R^2 values were created using the sjPlot package (see Lüdecke (2021) for details). The model statistics, p-values, standard errors and confidence intervals (CI; 95%) were computed using Satterthwaite's approximation for degrees of freedom. 'Plot no' is the plot identifier and 'tag' the tree identifier. All analyses were conducted in R version 4.1.2 (R Core Team, 2021).

Table S15 Best-fitting linear mixed-effects model of focal tree stomatal control traits after model selection.

	$\Delta\delta^{13}C$				
Predictors	*Estimates*	*CI*	*Statistic*	*p*	*df*
(Intercept)	0.36	0.16 – 0.56	3.61	**<0.001**	235.28
NSR	-0.04	-0.11 – 0.04	-0.93	0.351	239.44
year int	-0.15	-0.21 – -0.09	-4.76	**<0.001**	668.00
stomatal control	-0.29	-0.48 – -0.09	-2.84	**0.005**	228.98
NSR * year int	0.01	-0.02 – 0.03	0.51	0.610	668.00
NSR * stomatal control	0.09	0.01 – 0.16	2.26	**0.024**	315.29
year int * stomatal control	0.12	0.06 – 0.18	3.73	**<0.001**	668.00
(NSR * year int) * stomatal control	-0.03	-0.06 – -0.01	-2.66	**0.008**	668.00
Random Effects					
σ^2	0.15				
$\tau_{00\ tag:(plot\_no:site)}$	0.29				
$\tau_{00\ plot\_no:site}$	0.03				
ICC	0.68				
N_{tag}	336				
N_{plot_no}	114				
N_{site}	2				
Observations	1008				
Marginal R^2 / Conditional R^2	0.034 / 0.691				

Note: Significant fixed effects printed in bold. Linear mixed-effects models (LMMs) fit with the packages lme4 (Bates et al., 2015) and lmerTest (Kuznetsova et al., 2017) in R using restricted maximum likelihood estimation (REML) and an α of 0.05 for reporting significant effects. Model tables including fixed and random effects as well as R^2 values were created using the sjPlot package (see Lüdecke (2021) for details). The model statistics, p-values, standard errors and confidence intervals (CI; 95%) were computed using Satterthwaite's approximation for degrees of freedom. 'Plot no' is the plot identifier and 'tag' the tree identifier. All analyses were conducted in R version 4.1.2 (R Core Team, 2021).

Table S16 Best-fitting linear mixed-effects model of neighbour stomatal control traits after model selection.

	$\Delta\delta^{13}C$				
Predictors	*Estimates*	*CI*	*Statistic*	*p*	*df*
(Intercept)	0.28	0.19 – 0.37	5.90	**<0.001**	250.05
year int	-0.14	-0.17 – -0.11	-9.13	**<0.001**	670.00
stomatal control	-0.10	-0.20 – -0.01	-2.21	**0.028**	291.89
year int * stomatal control	0.05	0.02 – 0.08	3.43	**0.001**	670.00
Random Effects					
σ^2	0.15				
$\tau_{00\ tag:(plot\_no:site)}$	0.29				
$\tau_{00\ plot\_no:site}$	0.04				
ICC	0.68				
N_{tag}	336				
N_{plot_no}	114				
N_{site}	2				
Observations	1008				
Marginal R^2 / Conditional R^2	0.029 / 0.689				

Note: Significant fixed effects printed in bold. Linear mixed-effects models (LMMs) fit with the packages lme4 (Bates et al., 2015) and lmerTest (Kuznetsova et al., 2017) in R using restricted maximum likelihood estimation (REML) and an α of 0.05 for reporting significant effects. Model tables including fixed and random effects as well as R^2 values were created using the sjPlot package (see Lüdecke (2021) for details). The model statistics, p-values, standard errors and confidence intervals (CI; 95%) were computed using Satterthwaite's approximation for degrees of freedom. 'Plot no' is the plot identifier and 'tag' the tree identifier. All analyses were conducted in R version 4.1.2 (R Core Team, 2021).

Supplementary analysis 1

To test for potential differences between site A and B of the BEF-China experiment (Bruelheide et al., 2014), we conducted a separate analysis of *Schima superba*, the species sampled at both sites (Fig. 1, Table S1). We used the same linear mixed-effects model (LMMs) structure as in the main analyses but included site as fixed and not as random effect. LMMs thus modelled growth and $\delta^{13}C$ in response to focal tree size, competition by neighbours, climate, neighbourhood species richness (NSR) and site. We also included the 3-way interaction between climate × NSR × site as well as all potential 2-way interactions as fixed effects. We did not include species traits as we only examined one species. These analyses confirmed that growth and $\delta^{13}C$ responses did not differ between sites (see Tables S17,18 for the full models).

Table S17 Full linear mixed-effects model for growth of the species *Schima superba* exploring the influence of experimental site (A or B).

	log(bai_{std})				
Predictors	*Estimates*	*CI*	*Statistic*	*p*	*df*
(Intercept)	0.20	-0.15 – 0.54	1.16	0.256	30.49
dbh	0.22	0.13 – 0.32	4.83	**<0.001**	31.38
hegyi	-0.10	-0.19 – -0.01	-2.23	**0.033**	33.82
NSR	-0.09	-0.22 – 0.04	-1.46	0.153	34.34
year int	-0.15	-0.24 – -0.05	-3.15	**0.002**	80.00
site [B]	-0.18	-0.72 – 0.35	-0.74	0.472	13.16
NSR * year int	0.05	0.01 – 0.08	2.80	**0.006**	80.00
NSR * site [B]	0.05	-0.13 – 0.23	0.60	0.558	16.30
year int * site [B]	0.09	-0.04 – 0.22	1.37	0.174	80.00
(NSR * year int) * site [B]	-0.02	-0.07 – 0.03	-0.74	0.459	80.00
Random Effects					
σ^2	0.02				
$\tau_{00\ tag:plot\_no}$	0.05				
$\tau_{00\ plot\_no}$	0.01				
ICC	0.72				
N_{tag}	42				
N_{plot_no}	16				
Observations	126				
Marginal R^2 / Conditional R^2	0.468 / 0.854				

Note: Significant fixed effects printed in bold. Linear mixed-effects models (LMMs) fit with the packages lme4 (Bates et al., 2015) and lmerTest (Kuznetsova et al., 2017) in R using restricted maximum likelihood estimation (REML) and an α of 0.05 for reporting significant effects. Model tables including fixed and random effects as well as R^2 values were created using the sjPlot package (see Lüdecke (2021) for details). The model statistics, p-values, standard errors and confidence intervals (CI; 95%) were computed using Satterthwaite's approximation for degrees of freedom. All analyses were conducted in R version 4.1.2 (R Core Team, 2021).

Table S18 Full linear mixed-effects model for growth of the species *Schima superba* exploring the influence of experimental site (A or B).

	Δδ¹³C				
Predictors	*Estimates*	*CI*	*Statistic*	*p*	*df*
(Intercept)	0.20	-0.77 – 1.17	0.42	0.676	28.76
dbh	0.13	-0.09 – 0.35	1.18	0.247	27.81
hegyi	0.11	-0.11 – 0.33	1.04	0.305	30.79
NSR	0.03	-0.33 – 0.39	0.16	0.871	32.03
year int	-0.19	-0.45 – 0.07	-1.45	0.150	80.00
site [B]	0.66	-0.90 – 2.22	0.90	0.384	16.14
NSR * year int	0.02	-0.08 – 0.12	0.42	0.679	80.00
NSR * site [B]	-0.28	-0.82 – 0.25	-1.11	0.283	18.62
year int * site [B]	-0.05	-0.42 – 0.32	-0.26	0.795	80.00
(NSR * year int) * site [B]	0.04	-0.10 – 0.18	0.64	0.525	80.00
Random Effects					
σ^2	0.16				
$\tau_{00\ tag:plot\_no}$	0.21				
$\tau_{00\ plot\_no}$	0.15				
ICC	0.69				
N_{tag}	42				
N_{plot_no}	16				
Observations	126				
Marginal R^2 / Conditional R^2	0.078 / 0.713				

Note: Significant fixed effects printed in bold. Linear mixed-effects models (LMMs) fit with the packages lme4 (Bates et al., 2015) and lmerTest (Kuznetsova et al., 2017) in R using restricted maximum likelihood estimation (REML) and an α of 0.05 for reporting significant effects. Model tables including fixed and random effects as well as R^2 values were created using the sjPlot package (see Lüdecke (2021) for details). The model statistics, p-values, standard errors and confidence intervals (CI; 95%) were computed using Satterthwaite's approximation for degrees of freedom. All analyses were conducted in R version 4.1.2 (R Core Team, 2021).

Supplementary discussion 1 – coordination of drought-tolerance traits

We observed species responses in wet-to-dry years along the resistance-acquisition gradient consistent with the current understanding of a trade-off between high cavitation resistance (low Ψ_{50}) and acquisitive resource use in tropical tree species (Guillemot et al., 2022). Similarly, Reich (2014) concluded that acquisitive species thrive under optimal conditions due to their high capacity to transport and store water, while resistant species have slower resource economics but are less vulnerable to drought. Due to the orthogonality of the examined trait gradients, we interpret stomatal control as the extent to which early or late stomatal closure protects the tree's xylem from cavitation during drought at constant levels of cavitation resistance. We thus view stomatal control as a gradient capturing the trade-off between water spending (i.e. continued transpiration under drought) and water saving stomatal control (i.e. stomatal closure as protection against cavitation). This view aligns with contemporary perspectives (Martínez-Vilalta & Garcia-Forner, 2017) and fits the species responses we observed in wet-to-dry years.

However, some association between resistance-acquisition and stomatal control traits may be expected in general, as stomata regulate leaf water potentials to avoid xylem cavitation (McDowell et al., 2008). For instance, there is evidence that Ψ_{50} and the LES are associated with turgor loss point (arguably a proxy for stomatal control) and with (an-)isohydry across species (Fu & Meinzer, 2019; Klein, 2014; Zhu et al., 2018). In contrast, recent local studies did not find any relationship between turgor loss point and Ψ_{50} (Laughlin et al., 2020), nor between turgor loss point and LES traits (Maréchaux, Saint-André, Bartlett, Sack, & Chave, 2020). Therefore, the relationships between drought-tolerance traits likely depend on the geographical extent of the study and the range of traits considered. Particularly the multitude of approaches to quantify stomatal control and recent criticisms of classical approaches (Martínez-Vilalta & Garcia-Forner, 2017) may limit our ability to draw general conclusions on the nature and interrelation of both gradients. For instance, stomatal control defined as leaf water potential regulation (i.e. the classical (an-)isohydry definition) has been shown to be not strongly related to leaf gas exchange dynamics or the hydraulic or carbon limitations under drought (Martínez-Vilalta & Garcia-Forner, 2017). In this context, we consider direct measurements of stomatal conductance regulation (or similar ones like sap flux regulation; Schnabel et al., 2022) under gradients of soil and atmospheric drought as crucial to better characterize water-use and drought-tolerance strategies. Universal trait syndromes governing forest responses to drought thus remain controversial (e.g. Guillemot et al., 2022; Henry et al., 2019; Oliveira et al., 2021) and remain a research frontier for future studies.

References

Bates, D., Mächler, M., Bolker, B., & Walker, S. (2015). Fitting Linear Mixed-Effects Models Using lme4. *Journal of Statistical Software*, *67*(1). https://doi.org/10.18637/jss.v067.i01

Bruelheide, H., Nadrowski, K., Assmann, T., Bauhus, J., Both, S., Buscot, F., . . . Schmid, B. (2014). Designing forest biodiversity experiments: General considerations illustrated by a new large experiment in subtropical China. *Methods in Ecology and Evolution*, *5*(1), 74–89. https://doi.org/10.1111/2041-210X.12126

Fu, X., & Meinzer, F. C. (2019). Metrics and proxies for stringency of regulation of plant water status (iso/anisohydry): A global data set reveals coordination and trade-offs among water transport traits. *Tree Physiology*, *39*(1), 122–134. https://doi.org/10.1093/treephys/tpy087

Gärtner, H., & Nievergelt, D. (2010). The core-microtome: A new tool for surface preparation on cores and time series analysis of varying cell parameters. *Dendrochronologia*, *28*(2), 85–92. https://doi.org/10.1016/j.dendro.2009.09.002

Guillemot, J., Martin-StPaul, N., Bulascoschi, L., Poorter, L., Morin, X., Pinho, B. X., . . . Brancalion, P. H. S. (2022). Small and slow is safe: On the drought tolerance of tropical tree species. *Global Change Biology*. Advance online publication. https://doi.org/10.1111/gcb.16082

Harris, I., Osborn, T. J., Jones, P., & Lister, D. (2020). Version 4 of the CRU TS monthly high-resolution gridded multivariate climate dataset. *Scientific Data*, *7*(1), 109. https://doi.org/10.1038/s41597-020-0453-3

Henry, C., John, G. P., Pan, R., Bartlett, M. K., Fletcher, L. R., Scoffoni, C., & Sack, L. (2019). A stomatal safety-efficiency trade-off constrains responses to leaf dehydration. *Nature Communications*, *10*(1), 3398. https://doi.org/10.1038/s41467-019-11006-1

Huang, Y., Chen, Y., Castro-Izaguirre, N., Baruffol, M., Brezzi, M., Lang, A., . . . Schmid, B. (2018). Impacts of species richness on productivity in a large-scale subtropical forest experiment. *Science*, *362*(6410), 80–83. https://doi.org/10.1126/science.aat6405

Klein, T. (2014). The variability of stomatal sensitivity to leaf water potential across tree species indicates a continuum between isohydric and anisohydric behaviours. *Functional Ecology*, *28*(6), 1313–1320. https://doi.org/10.1111/1365-2435.12289

Kröber, W., & Bruelheide, H. (2014). Transpiration and stomatal control: a cross-species study of leaf traits in 39 evergreen and deciduous broadleaved subtropical tree species. *Trees*, *28*(3), 901–914. https://doi.org/10.1007/s00468-014-1004-3

Kröber, W., Zhang, S., Ehmig, M., & Bruelheide, H. (2014). Linking xylem hydraulic conductivity and vulnerability to the leaf economics spectrum--a cross-species study of 39 evergreen and deciduous broadleaved subtropical tree species. *PLoS ONE*, *9*(11), e109211. https://doi.org/10.1371/journal.pone.0109211

Kuznetsova, A., Brockhoff, P. B., & Christensen, R. H. B. (2017). lmerTest Package: Tests in Linear Mixed Effects Models. *Journal of Statistical Software*, *82*(13). https://doi.org/10.18637/jss.v082.i13

Laughlin, D. C., Delzon, S., Clearwater, M. J., Bellingham, P. J., McGlone, M. S., & Richardson, S. J. (2020). Climatic limits of temperate rainforest tree species are explained by xylem embolism resistance among angiosperms but not among conifers. *New Phytologist*, *226*(3), 727–740. https://doi.org/10.1111/nph.16448

Lüdecke, D. (2021). sjPlot: Data Visualization for Statistics in Social Science [Computer software]. Retrieved from https://CRAN.R-project.org/package=sjPlot

Mailly, D., Turbis, S., & Pothier, D. (2003). Predicting basal area increment in a spatially explicit, individual tree model: a test of competition measures with black spruce. *Canadian Journal of Forest Research*, *33*(3), 435–443. https://doi.org/10.1139/X02-122

Maréchaux, I., Saint-André, L., Bartlett, M. K., Sack, L., & Chave, J. (2020). Leaf drought tolerance cannot be inferred from classic leaf traits in a tropical rainforest. *Journal of Ecology*, *108*(3), 1030–1045. https://doi.org/10.1111/1365-2745.13321

Martínez-Vilalta, J., & Garcia-Forner, N. (2017). Water potential regulation, stomatal behaviour and hydraulic transport under drought: Deconstructing the iso/anisohydric concept. *Plant, Cell and Environment*, *40*(6), 962–976. https://doi.org/10.1111/pce.12846

McDowell, N. G., Pockman, W. T., Allen, C. D., Breshears, D. D., Cobb, N., Kolb, T., . . . Yepez, E. A. (2008). Mechanisms of plant survival and mortality during drought: Why do some plants survive while others succumb to drought? *New Phytologist*, *178*(4), 719–739. https://doi.org/10.1111/j.1469-8137.2008.02436.x

Oliveira, R. S., Eller, C. B., Barros, F. d. V., Hirota, M., Brum, M., & Bittencourt, P. (2021). Linking plant hydraulics and the fast-slow continuum to understand resilience to drought in tropical ecosystems. *New Phytologist*, *230*(3), 904–923. https://doi.org/10.1111/nph.17266

R Core Team (2021). A language and environment for statistical computing [Computer software]. Vienna, Austria: R Foundation for Statistical Computing: R Foundation for Statistical Computing. Retrieved from https://www.R-project.org/

Reich, P. B. (2014). The world-wide ‘fast-slow’ plant economics spectrum: a traits manifesto. *Journal of Ecology*, *102*(2), 275–301. https://doi.org/10.1111/1365-2745.12211

Schnabel, F., Liu, X., Kunz, M., Barry, K. E., Bongers, F. J., Bruelheide, H., . . . Wirth, C. (2021). Species richness stabilizes productivity via asynchrony and drought-tolerance diversity in a large-scale tree biodiversity experiment. *Science Advances*, *7*(51). https://doi.org/10.1126/sciadv.abk1643

Schnabel, F., Purrucker, S., Schmitt, L., Engelmann, R. A., Kahl, A., Richter, R., . . . Wirth, C. (2022). Cumulative growth and stress responses to the 2018-2019 drought in a European floodplain forest. *Global Change Biology*, *28*(5), 1870–1883. https://doi.org/10.1111/gcb.16028

Vicente-Serrano, S. M., Beguería, S., & López-Moreno, J. I. (2010). A Multiscalar Drought Index Sensitive to Global Warming: The Standardized Precipitation Evapotranspiration Index. *Journal of Climate*, *23*(7), 1696–1718. https://doi.org/10.1175/2009JCLI2909.1

Zhu, S.-D., Chen, Y.-J., Ye, Q., He, P.-C., Liu, H., Li, R.-H., . . . Cao, K.-F. (2018). Leaf turgor loss point is correlated with drought tolerance and leaf carbon economics traits. *Tree Physiology*, *38*(5), 658–663. https://doi.org/10.1093/treephys/tpy013